Single-FOV Uncertainty Estimates of the VIIRS+CrIS Fusion Radiance Products

E. Eva Borbas, Elisabeth Weisz, Dongwei Fu, W. Paul Menzel, Chris Moeller, Geoff Cureton*, Greg Quinn*

Space Science and Engineering Center, University of Wisconsin-Madison

**NASA Atmosphere-SIPS*

Outline

- Fusion method
- Data monitoring, evaluation
- Single-FOV uncertainty estimates
- Future Plans

Goal

- The VIIRS+CrIS Fusion Radiance (FSNRAD) products have been created to provide a path for continuity of products based on the Terra, Aqua, SNPP, and NOAA-20 platforms.

- *Why is this work important?* MODIS has three channels sensitive to CO_2 in the 4.5 µm CO_2 band, four channels in the broad 15 µm CO_2 band, 2 channels sensitive to H_2O near 6.7 µm, and an ozone channel near 9 µm. VIIRS has none of these IR absorption bands. The lack of the CO_2 and H_2O channels results in a degradation of the accuracy of the cloud mask especially at night in high latitudes, other cloud products (cloud top pressure/height and thermodynamic phase) and the moisture products (total precipitable water vapor, upper tropospheric humidity).

- We addressed this restriction by constructing similar Aqua MODIS IR band radiances for VIIRS based on a fusion method that uses collocated VIIRS and CrIS data.

Imager+Sounder Spatial Fusion Schematics

Step 1

Imager geolocation
HIRES Imager radiances
(imager bands X and Y)

Sounder geolocation

Collocation and Geographic Averaging

Sounder geolocation
LORES Imager radiances
(imager bands X and Y)

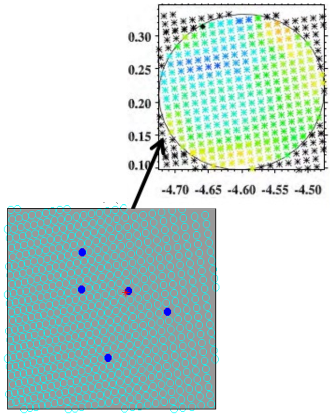

K-D Search Tree *(Bentley, 1975)*

N=5 Indices of N closest sounder FOVs
(for each imager pixel)

Step 2

Radiance Fusion

LORES Sounder Radiance
Convolved to Band Z

Average N Sounder FOVs
(for each imager pixel)

HIRES Fusion Radiance
At Imager Band Z

LORES/HIRES … low/high spatial resolution

(Cross et al. 2013, Weisz et al. 2017)

VIIRS+CrIS FSNRAD Product (on full VIIRS spatial resolution)

MODIS Infrared bands		VIIRS+CrIS Fusion Infrared bands		Primary Use
band	Central Wavelength [µm]	band	Central Wavelength [µm]	
23	4.05	M13	4.05	Atmospheric temperature
24	4.47	M24 Fusion	4.47	Atmospheric temperature
25	4.52	M25 Fusion	4.52	Atmospheric temperature
27	6.72	M27 Fusion*	6.72	Water vapor
28	7.33	M28 Fusion	7.33	Water vapor
29	8.55	M14	8.55	Surface and cloud properties
30	9.73	M30 Fusion	9.73	Ozone
31	11.03	M15 M15 Fusion**	10.76	Surface and cloud properties
32	12.02	M16 M16 Fusion**	12.01	Surface and cloud properties
33	13.34	M33 Fusion*	13.34	Cloud properties
34	13.64	M34 Fusion*	13.64	Cloud properties
35	13.94	M35 Fusion*	13.94	Cloud properties
36	14.23	M36 Fusion*	14.23	Cloud properties

*FSNRAD_SS subset for the CERES team – through Langley ASDC

**BT diff for M15 and M16 are also provided for uncertainty estimate

Status of the V2 VIIRS+CrIS FSNRAD products

Product Name	Description	Status	Available at
FSNRAD_L2_VIIRS_CRIS_SNPP	S-NPP/VIIRS Fusion Radiances	Operational	LAADS DAAC
FSNRAD_L2_VIIRS_CRIS_NOAA20	NOAA20/VIIRS Fusion Radiances	Operational	LAADS DAAC
FSNRAD_L2_VIIRS_CRIS_SS_SNPP	S-NPP/VIIRS Subsetted Fusion Radiances	Operational	Atmosphere-SIPS
FSNRAD_L2_VIIRS_CRIS_SS_NOAA20	NOAA20/VIIRS Subsetted Fusion Radiances	Operational	Atmosphere-SIPS
FSNRAD_L2_VIIRS_CRIS_NOAA21	NOAA21/VIIRS Fusion Radiances	Tested	
FSNRAD_L2_VIIRS_CRIS_SS_NOAA21	NOAA21/VIIRS Subsetted Fusion Radiances	Tested	

- **V2 FSNRAD available at NASA LAADS DAAC:**
  - DOI: 10.5067/VIIRS/FSNRAD_L2_VIIRS_CRIS_SNPP.002
  - DOI: 10.5067/VIIRS/FSNRAD_L2_VIIRS_CRIS_NOAA20.002

- **Note for SNPP:** CrIS anomaly in LW data
  - May 21, 2021 – July 12, 2021: fill value for Band 30-36 (anomaly of CrIS LW channels)
  - July 14, 2021 - Aug 29, 2023: fill value for Band 27, 28,
  - B30-36 restored (Side 1 -> Side 2)
  - Aug 29, 2023 - Aug 31, 2023: fill value for Band 27-36 (Side 2 LW failure, MW was not working already)
  - Aug 31/Sept 8 (operational), 2023 - fill value for Band 30-36, but B27, 28 restored (Side 2- Side 1)

Routine Assessment of Product Quality: Mean of BTdiffs (N20 FSNRAD –Aqua/MODIS)

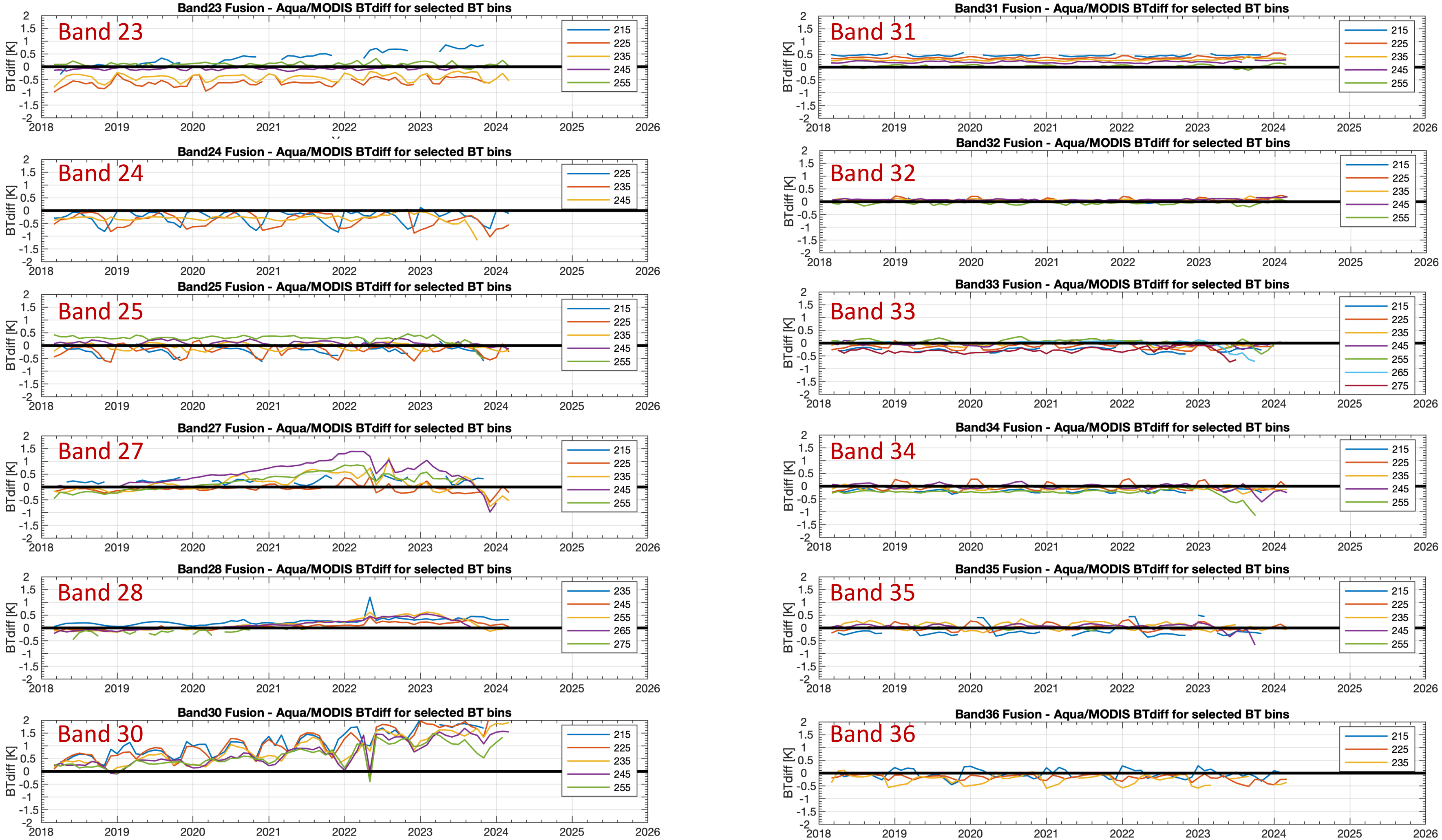

Routine Assessment of Product Quality: STDEV of BT diffs (N20 FSNRAD –Aqua/MODIS)

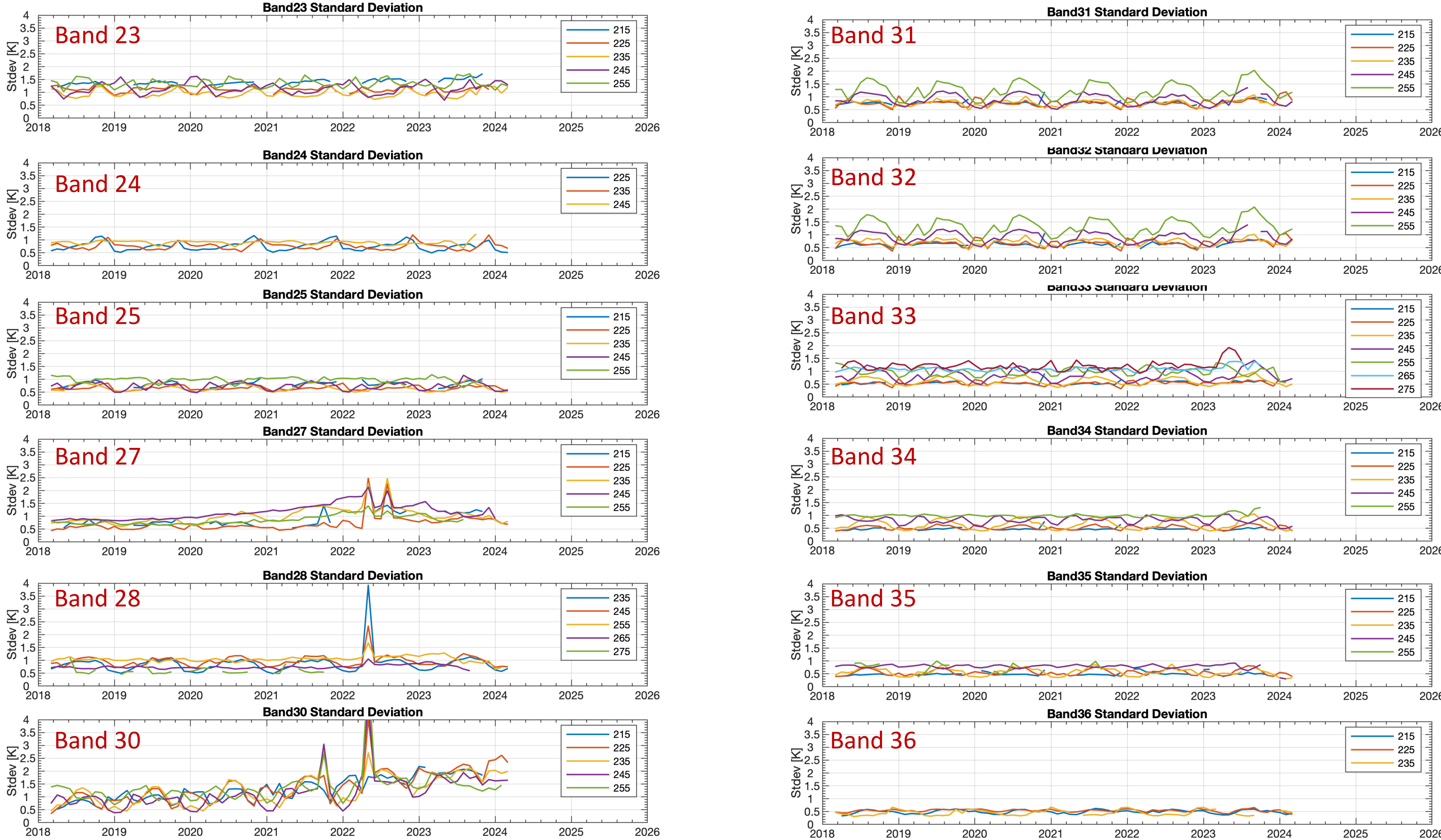

Routine Assessment of Product Quality: Sample Numbers (N20 FSNRAD –Aqua/MODIS)

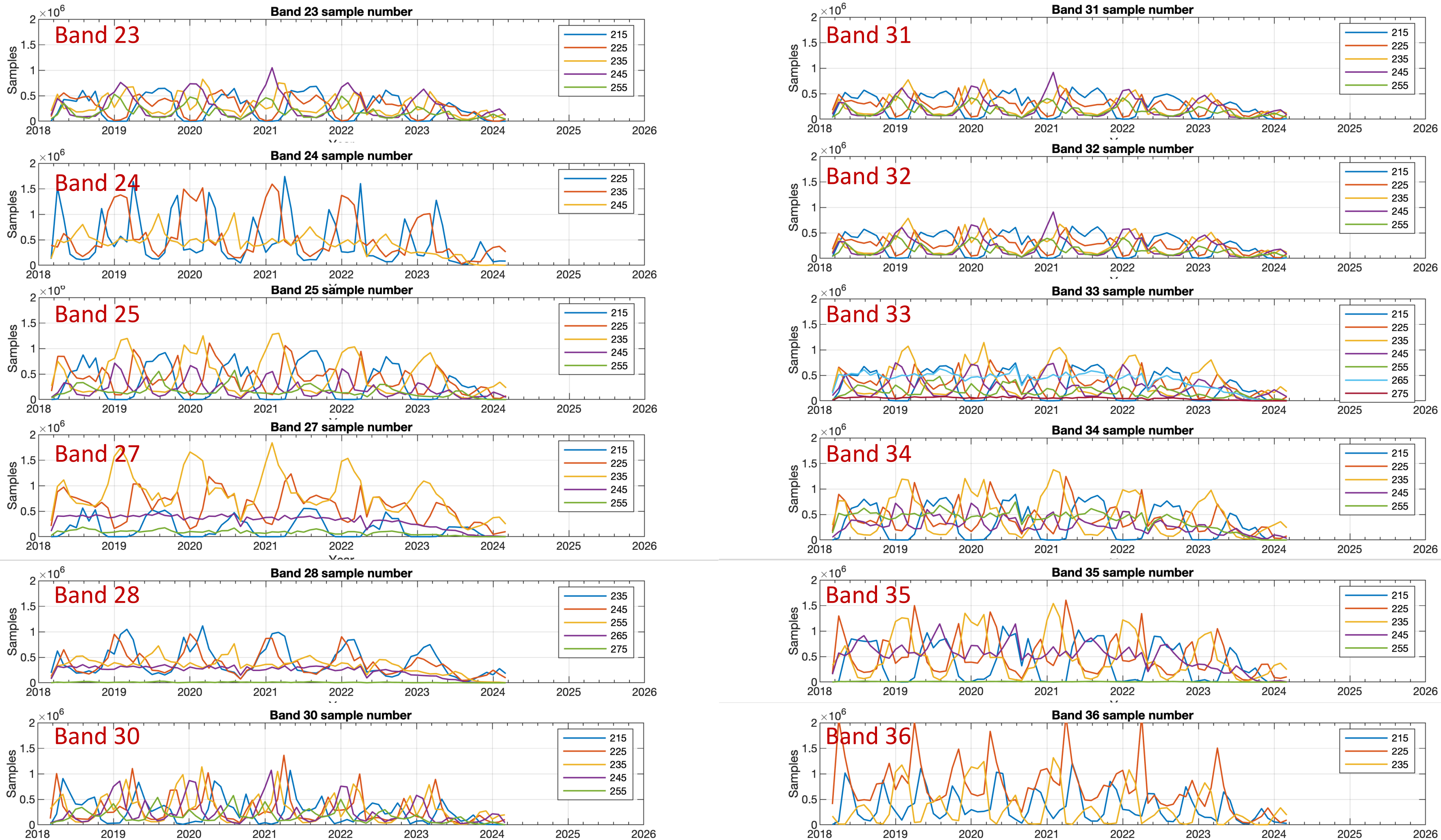

Evaluation in Cloud Mask with CALIOP for 2014

Definition: CALIOP: cloudy if OD > 0.2, otherwise clear
MOD35/MVCM: clear if probably or confident clear
cloudy if probably or confident cloudy

Monthly mean agreements over the South Pole

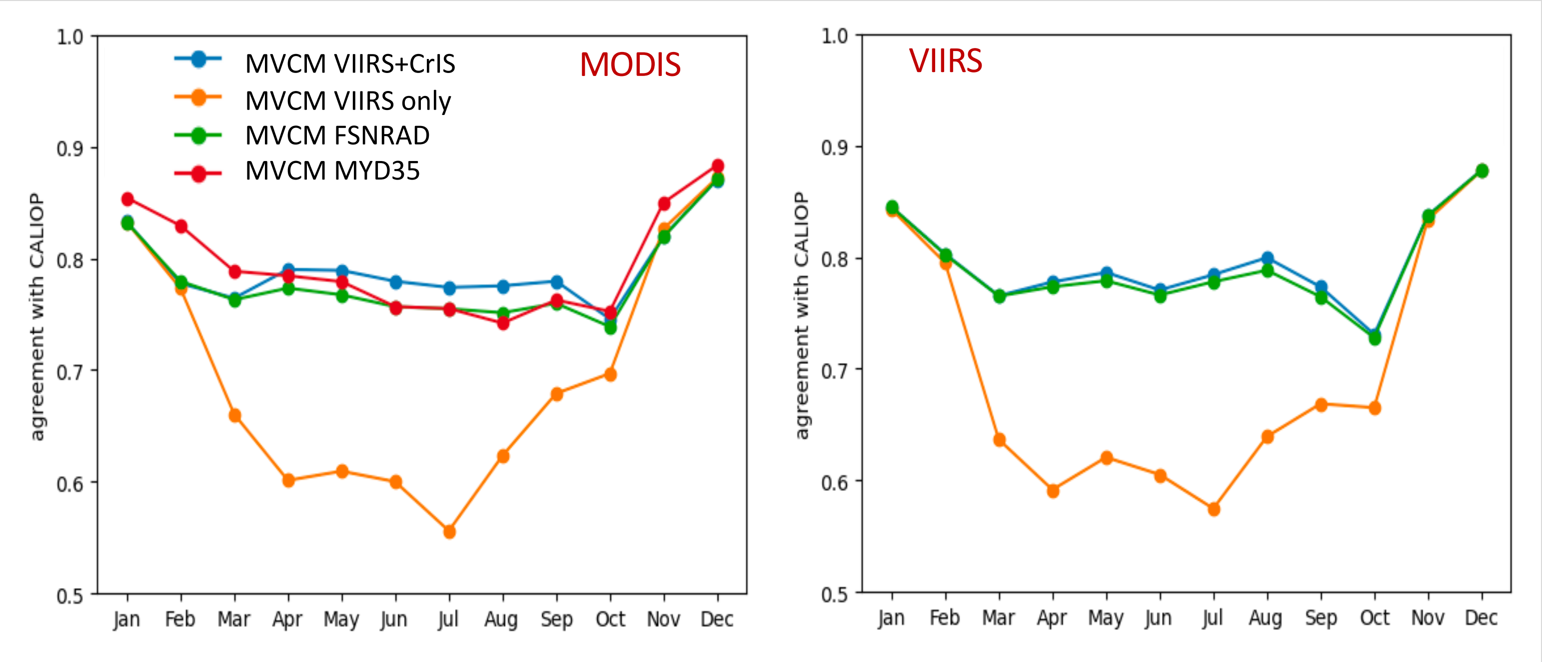

(Li et al. 2020) used the 6.7 and 13.3 μm CrIS+VIIRS fusion bands in CLAVR-X, the NOAA operational cloud processing package. They demonstrated that the fusion radiancies improved cloud parameters, *like cloud mask (polar regions), type/phase, and cloud height for all latitudes.*

Determining Single-FOV Uncertainties

- The goal was to provide a methodology to calculate uncertainties for each band of the V2 FSNRAD products

- Developed on MODIS+AIRS
- Applied on VIIRS+CrIS

BT [K] Statistics of MODIS/AIRS Fusion (April 17, 2015, global) – VIIRS/CrIS Fusion (Red)

	Full swath			Sounder swath		
	Mean	Stdev	RMS	Mean	Stdev	RMS
Band 23	-0.23	2.35	2.36	-0.11	1.95	1.95
Band 24	0.34	1.10	1.16	0.38	0.97	1.05
Band 25	-0.33	1.15	1.20	-0.20	0.83	0.85
Band 27	-0.15	2.02	2.03	-0.07	1.69	1.69
Band 28	-0.37	3.04	3.06	-0.26	2.60	2.62
Band 30	0.29	1.09	1.13	0.43	0.77	0.88
Band 31	-0.18	1.41	1.42	-0.13	0.89	0.90
Band 32	-0.16	1.40	1.41	-0.12	0.88	0.89
Band 33	-0.24	1.11	1.14	-0.14	0.79	0.80
Band 34	0.14	1.00	1.01	0.25	0.72	0.76
Band 35	-0.16	0.81	0.83	-0.08	0.61	0.61
Band 36	0.11	0.56	0.57	0.10	0.48	0.47
Band 15	0.08	1.00	1.00	0.14	0.56	0.58
Band 16	-0.11	0.94	0.95	0.05	0.45	0.45

Methodology to derive SFOV VIIRS/CRIS Fusion 'OBT-FBT' BTD estimates

STEP 1: Derive the least-square solution coefficients between the observed – fusion BT differences for each channel and the predictors. MODIS and MODIS/AIRS fusion BT data are used for the full path (Matlab code: LSCOV).

Four Variables (predictors): [1] MODIS split-window (Band 31, Band 32) BT differences,

[2] Band 31 Observed minus Fusion BTs,

[3] Band 32 Observed minus Fusion BTs,

[4] MODIS Satellite zenith angle

	land				sea			
bands	Coef1	Coef2	Coef3	Coef4	Coef1	Coef2	Coef3	Coef4
23	-0.1350	2.1651	-1.3409	0.0051	-0.0213	2.7231	-1.8469	-0.0065
24	0.1606	-0.2468	0.3233	0.0108	0.0144	-0.0933	0.2229	0.0058
25	-0.0006	0.6346	-0.0946	-0.0055	-0.0142	0.7189	-0.1439	-0.0082
27	-0.0391	-0.0851	0.5645	-0.0003	-0.1736	-0.0227	0.5993	-0.0005
28	0.0197	0.0044	1.0031	-0.0081	0.0571	-0.2826	1.3784	-0.0067
30	0.1364	0.6077	-0.1452	0.0082	0.2000	0.7332	-0.2311	0.0002
31	0	1	0	0	0	1	0	0
32	0	0	1	0	0	0	1	0
33	0.0027	-0.6151	1.1610	-0.0058	0.0004	-0.7261	1.2984	-0.0055
34	0.0560	-0.7113	1.0267	0.0034	0.0508	-0.7486	1.1021	0.0002
35	-0.0078	-0.5134	0.7384	-0.0033	-0.0305	-0.5552	0.8117	-0.0046
36	-0.0381	-0.2538	0.3323	0.0050	-0.0494	-0.2760	0.3706	0.0039

Methodology to derive SFOV VIIRS/CRIS Fusion 'OBT-FBT' BTD estimates (Cont.)

STEP 2: . Apply these coefficients to original VIIRS B15 and B16 BTs and OBT-FBT BTD (from V/C fusion *nc files) for each fusion (MODIS) band:

xy = [pred1, pred2, pred3, pred4]

vc_btd = xy *coeffs

Where,

vc_btd … final V/C fusion BTD estimates
coeffs … coefficients from table [4x2]
pred1 … VIIRS B15-B16 BTs
pred2, pred3 … V/C Band 15 and Band 16 OBT-FUSION BTD, respectively
pred 4 … VIIRS satellite zenith angle

Case study
(mostly over ocean) on 4/17/2015

MODIS granule: at 1435 UTC

VIIRS granules: at 1436 and 1442 UTC

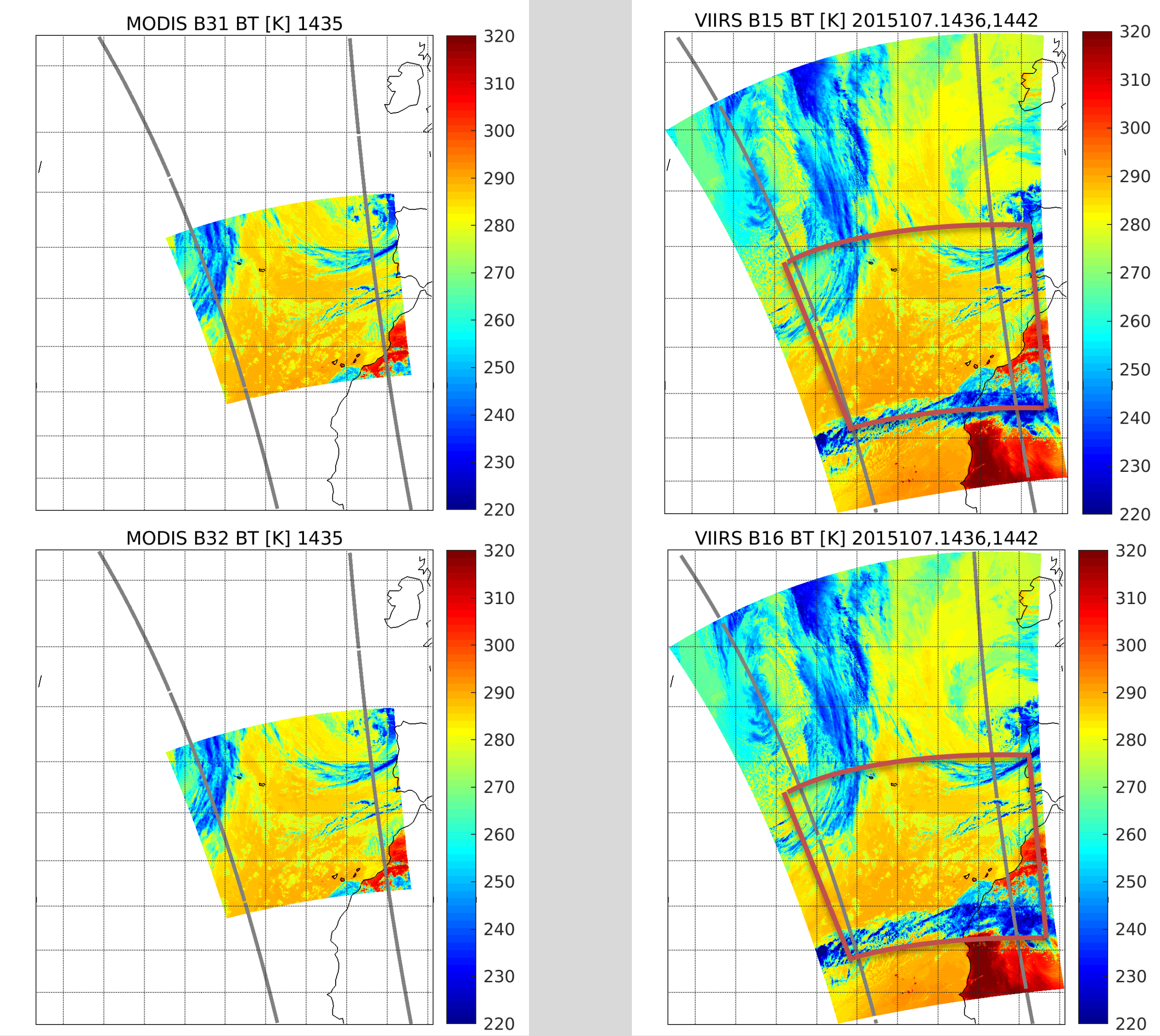
MODIS B31 BT [K] 1435
VIIRS B15 BT [K] 2015107.1436,1442
MODIS B32 BT [K] 1435
VIIRS B16 BT [K] 2015107.1436,1442
320
310
300
290
280
270
260
250
240
230
220

Predictor 1

MODIS B31 – B32 BT Diff [K]

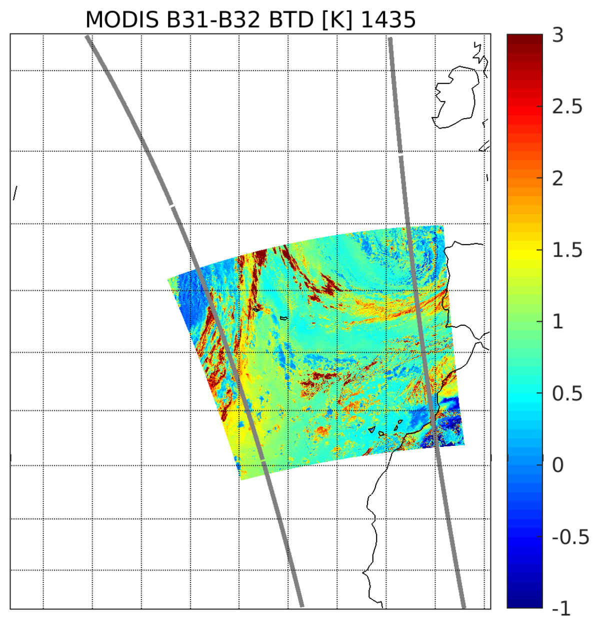

VIIRS M15 – M16 BT Diff [K]

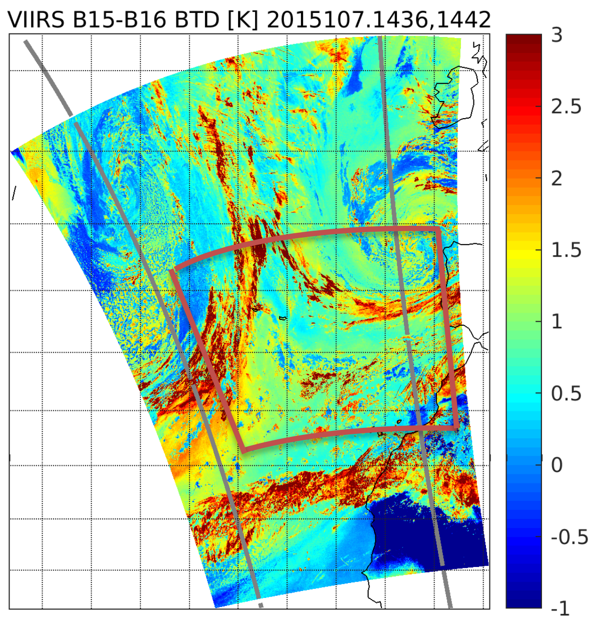

Predictor 2 & 3

Band M15 Observed – Fusion BT [K]

Band M16 Observed – Fusion BT [K]

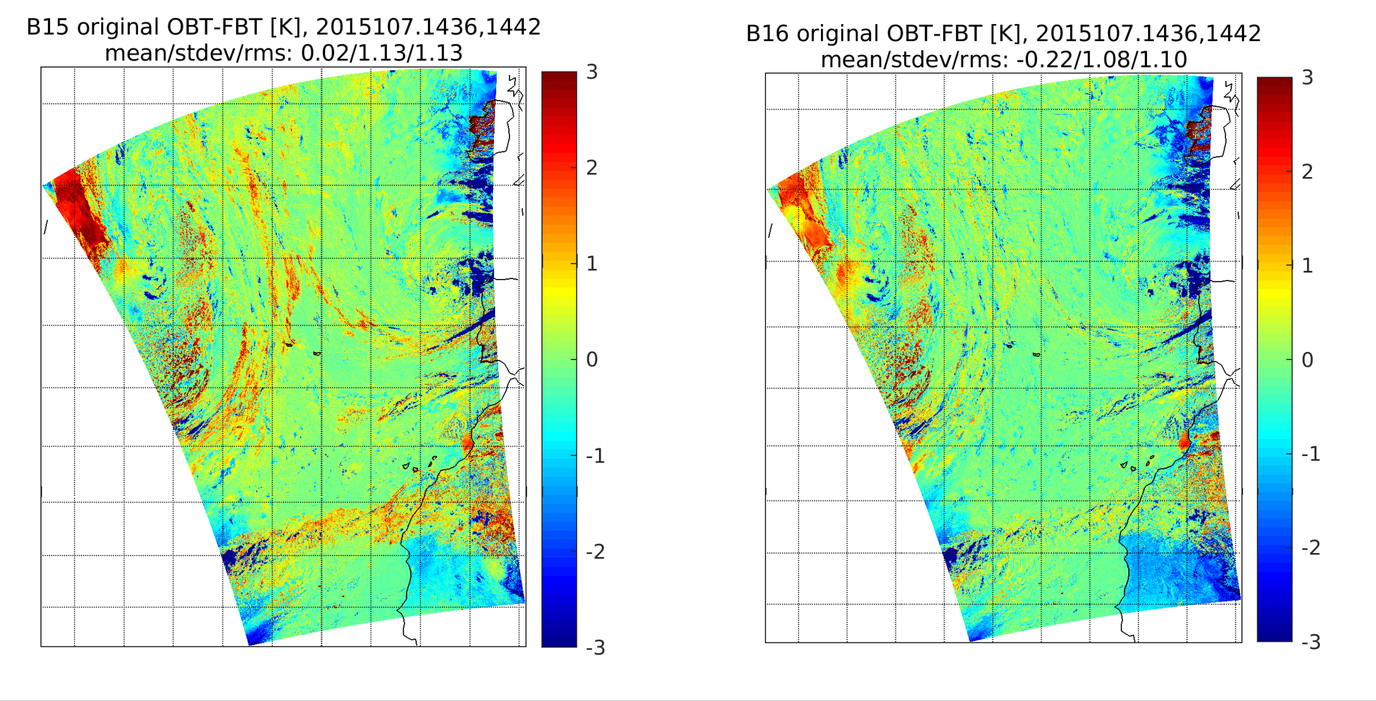

*This data includes the FSNRAD product files.

Band 31 MODIS/AIRS and VIIRS/CrIS Fusion OBT-FBT [K]

MODIS/AIRS OBT-FBT [K]

VIIRS/CrIS OBT-FBT [K]

Original O-F BTs

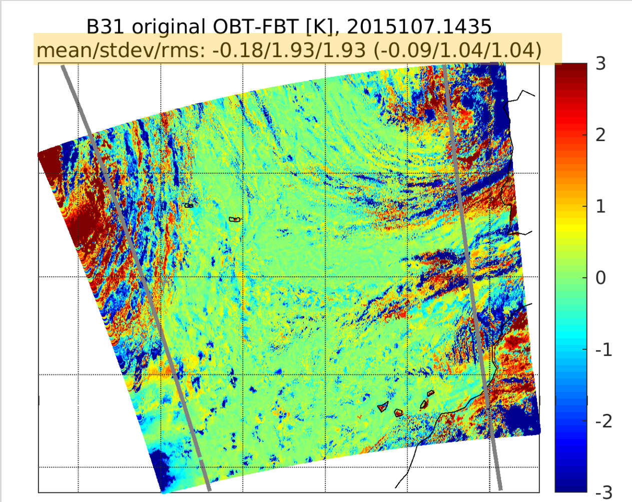

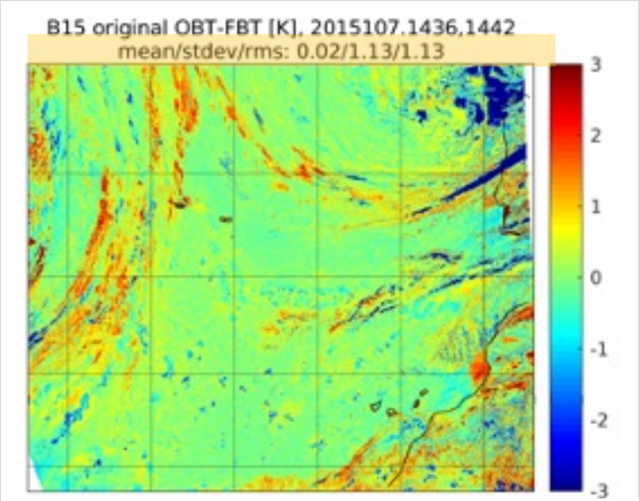

Estimated O-F BTs

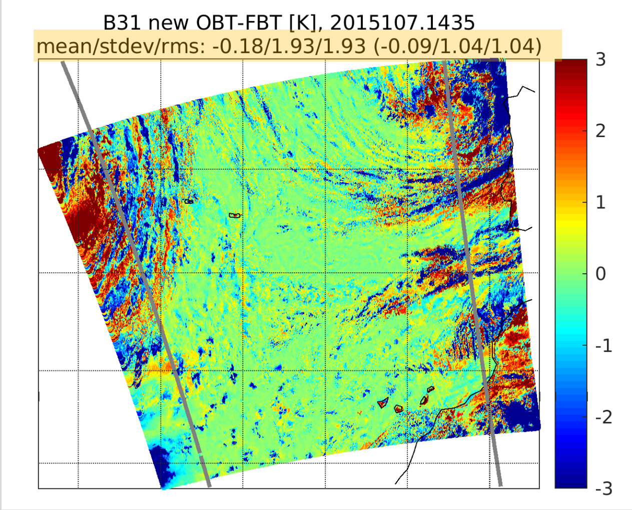

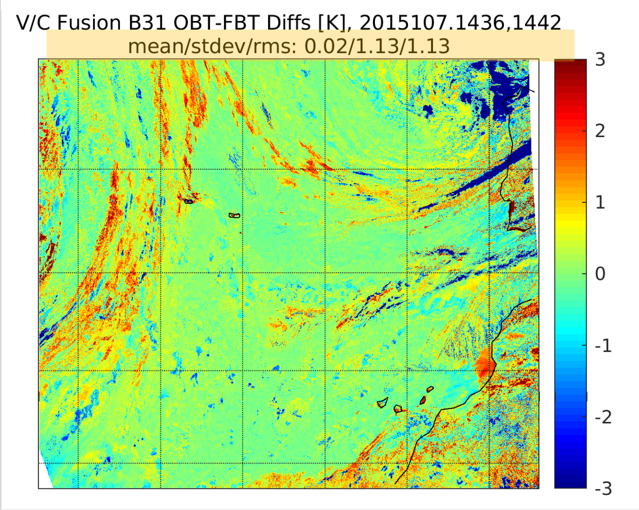

Band 27 MODIS/AIRS and VIIRS/CrIS Fusion OBT-FBT [K]

MODIS/AIRS OBT-FBT [K]

VIIRS/CrIS OBT-FBT [K]

Original
O-F BTs

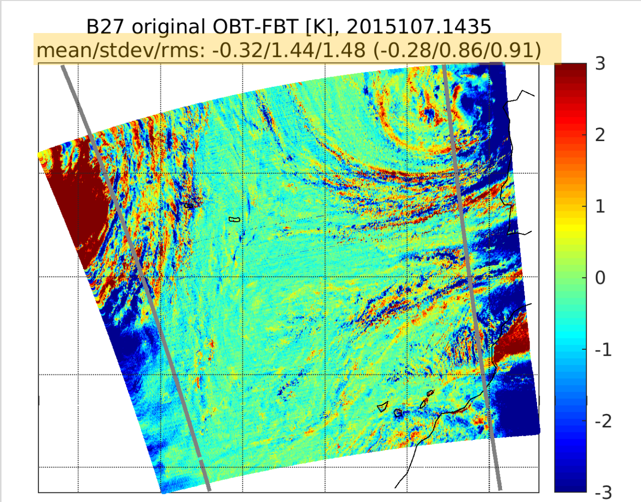

Full
granule

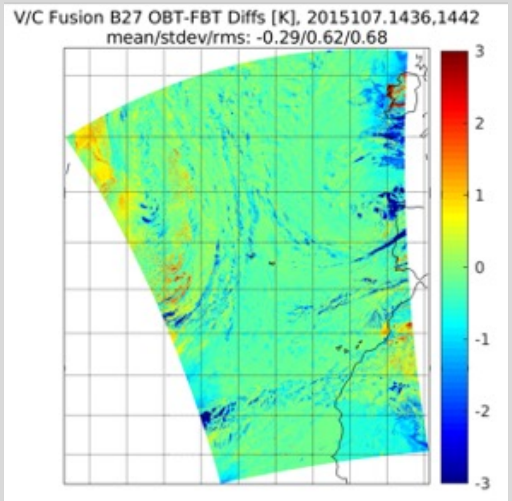

Estimated
O-F BTs

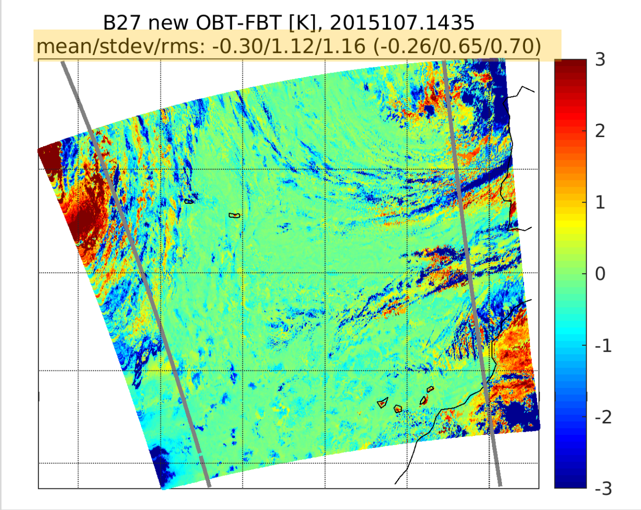

Subset

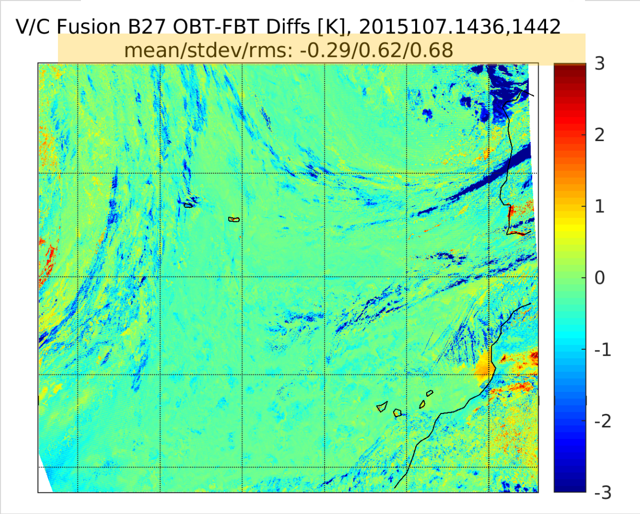

Band 33 MODIS/AIRS and VIIRS/CrIS Fusion OBT-FBT [K]

MODIS/AIRS OBT-FBT [K]

VIIRS/CrIS OBT-FBT [K]

Original
O-F BTs

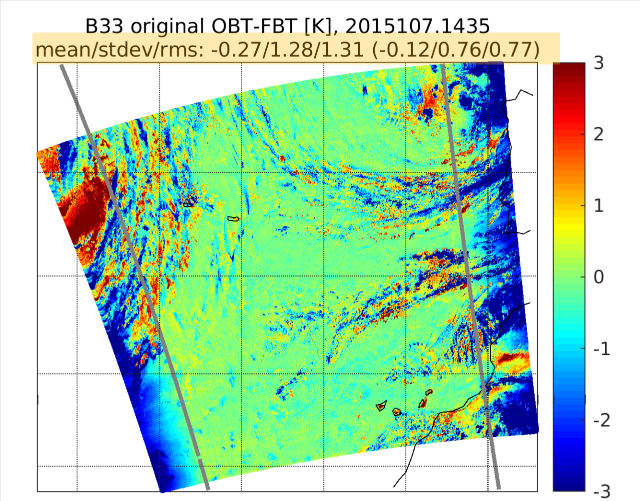

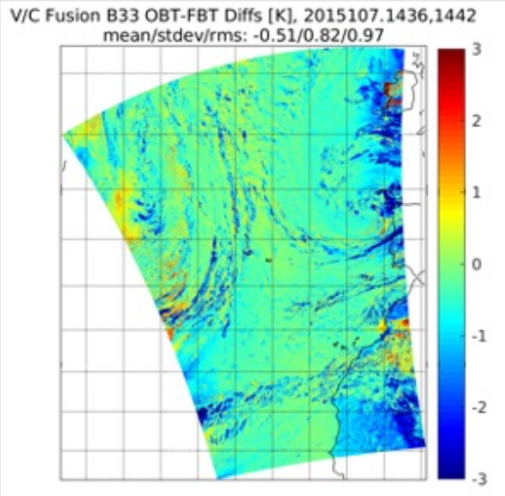

Full
granule

Estimated
O-F BTs

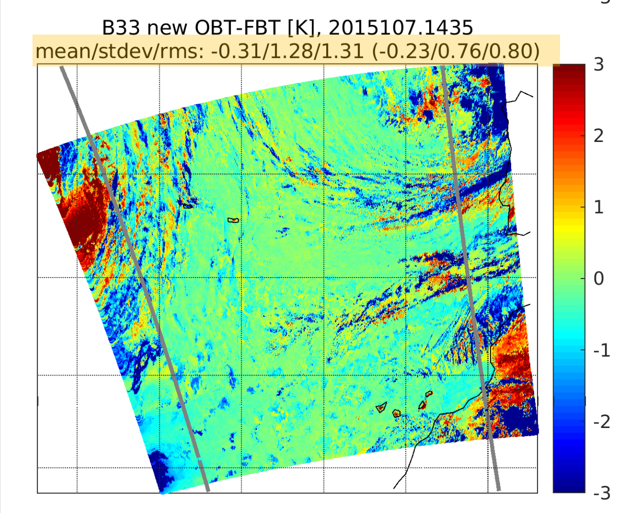

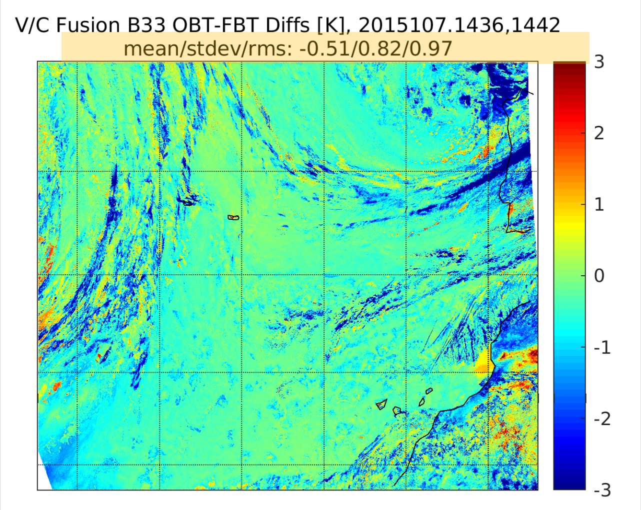

Subset

Band 34 MODIS/AIRS and VIIRS/CrIS Fusion OBT-FBT [K]

MODIS/AIRS OBT-FBT [K]

VIIRS/CrIS OBT-FBT [K]

Original O-F BTs

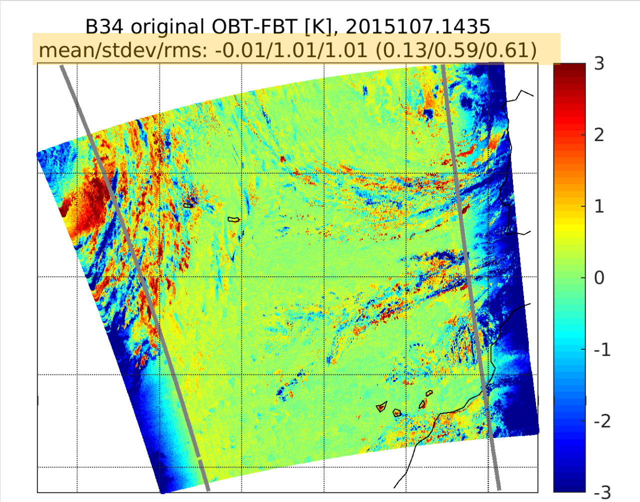

Full granule

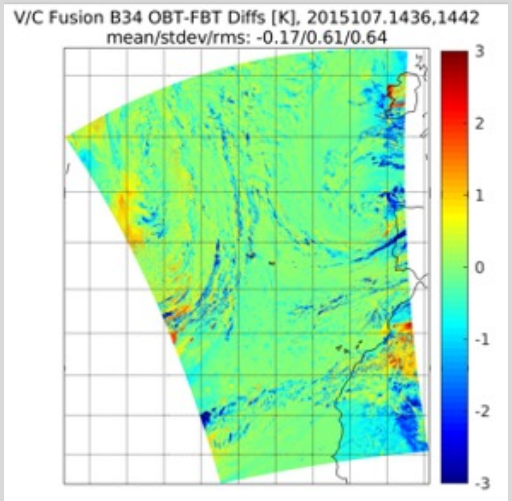

Estimated O-F BTs

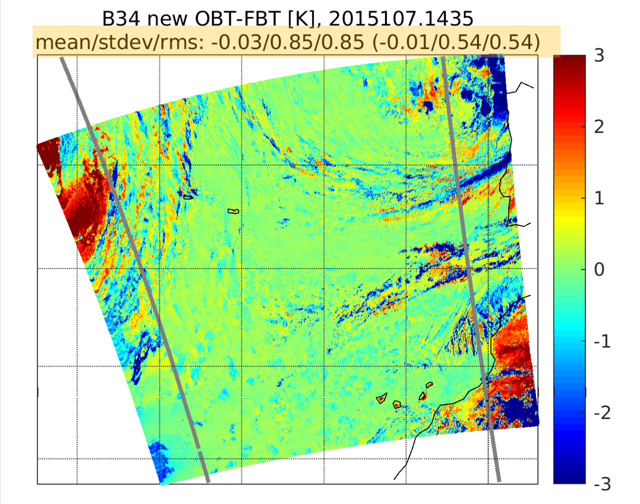

Subset

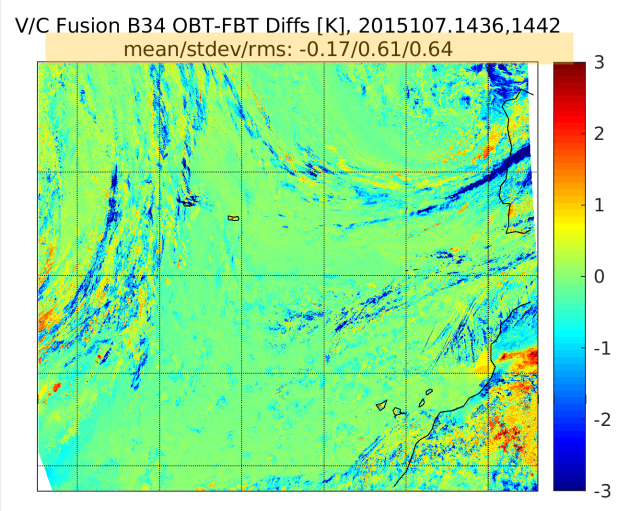

Band 36 MODIS/AIRS and VIIRS/CrIS Fusion OBT-FBT [K]

MODIS/AIRS OBT-FBT [K]

VIIRS/CrIS OBT-FBT [K]

Original O-F BTs

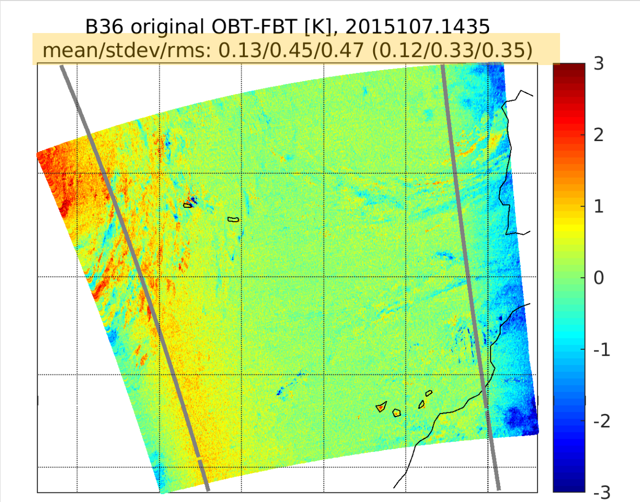

Full granule

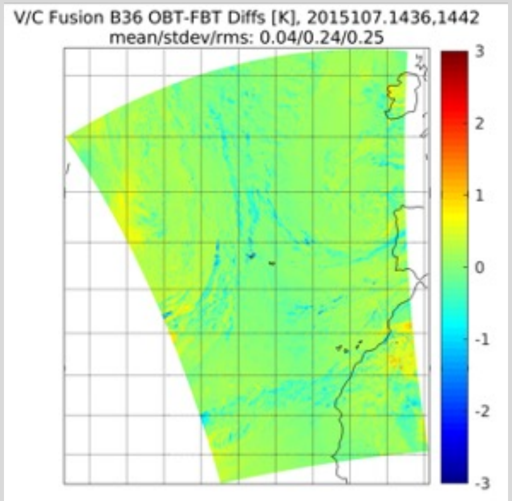

Estimated O-F BTs

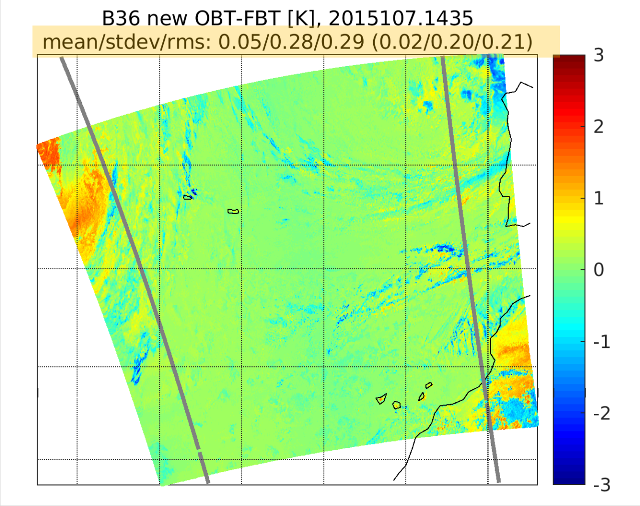

Subset

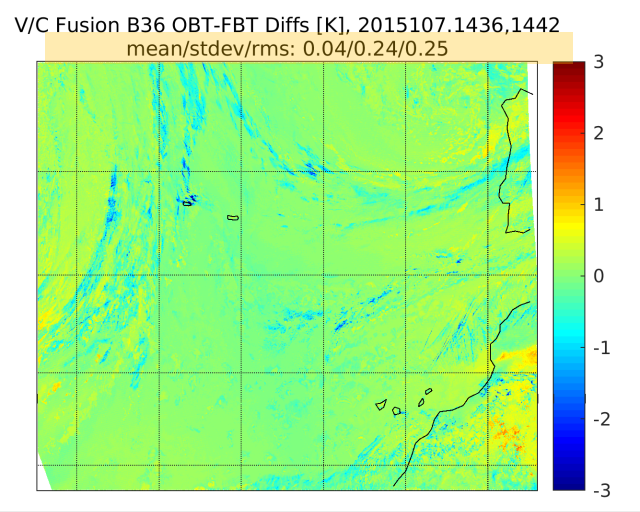

Comparison of the MODIS and VIIRS Split Window Band Differences

Compute global statistics from
convolved (1) AIRS to MODIS and (2) AIRS to VIIRS split-window band differences
for every FOV in every granule on 04/17/2015

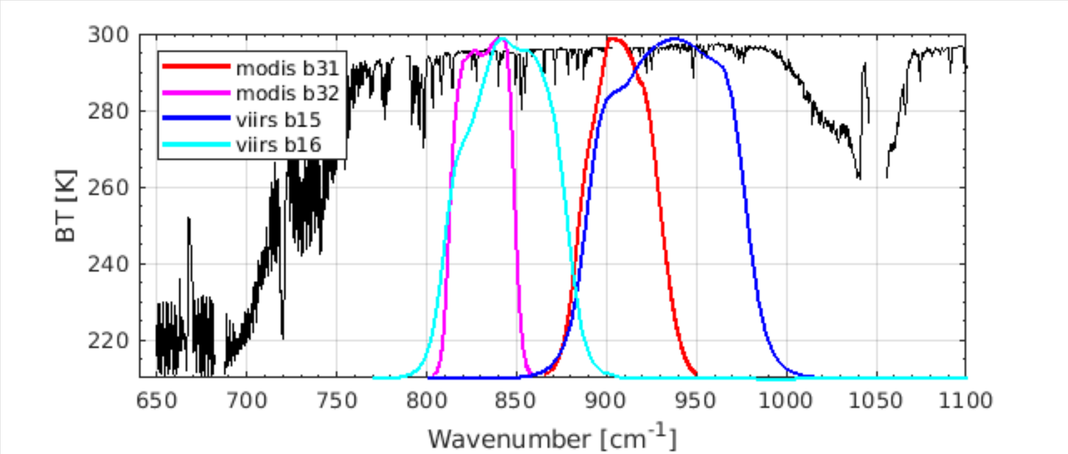

AIRS convolved to MODIS B31-B32 BTD (mean, stdev, rms=0.779, 0.950, 1.228 K)

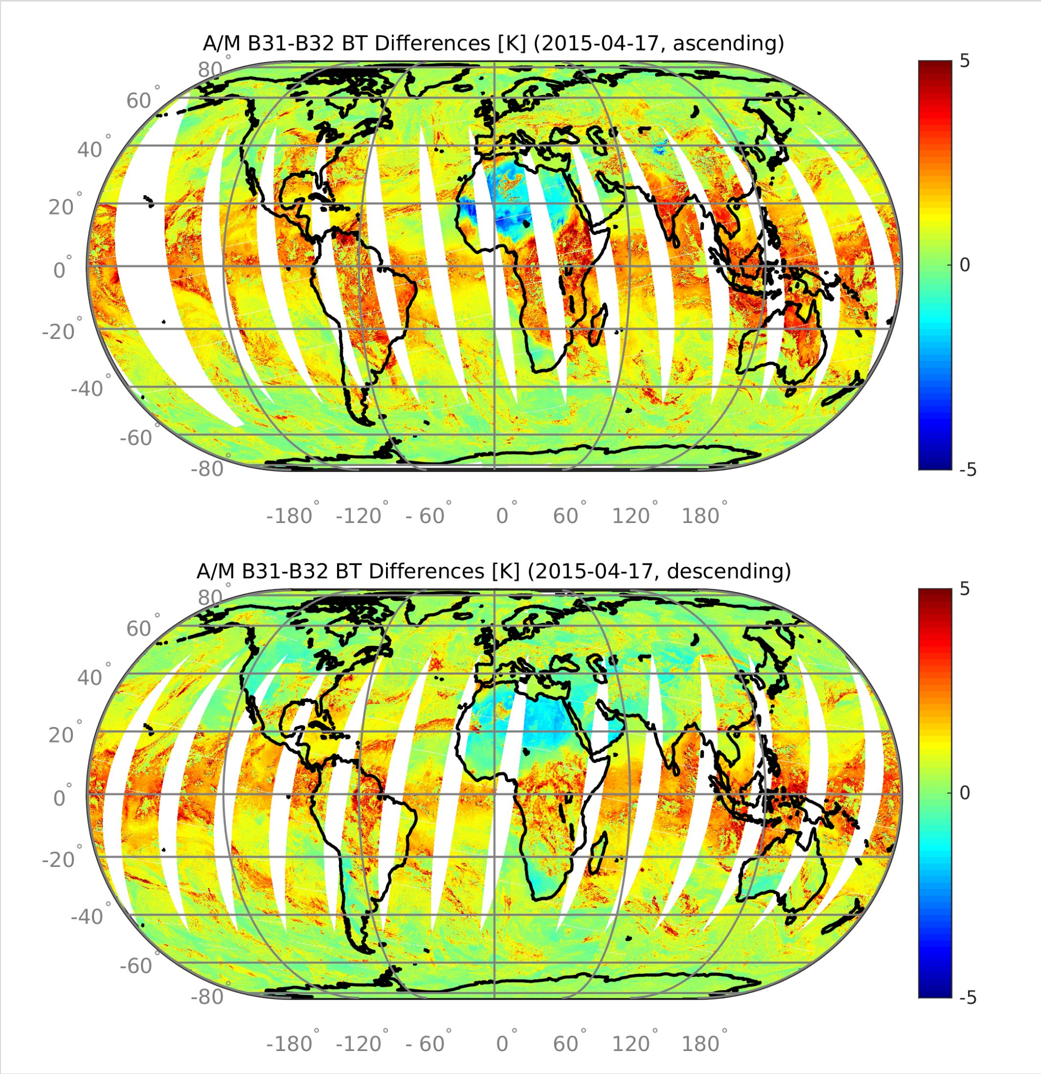

AIRS convolved VIIRS B15-B16 BTD (mean, stdev, rms=0.957, 1.036, 1.411 K)

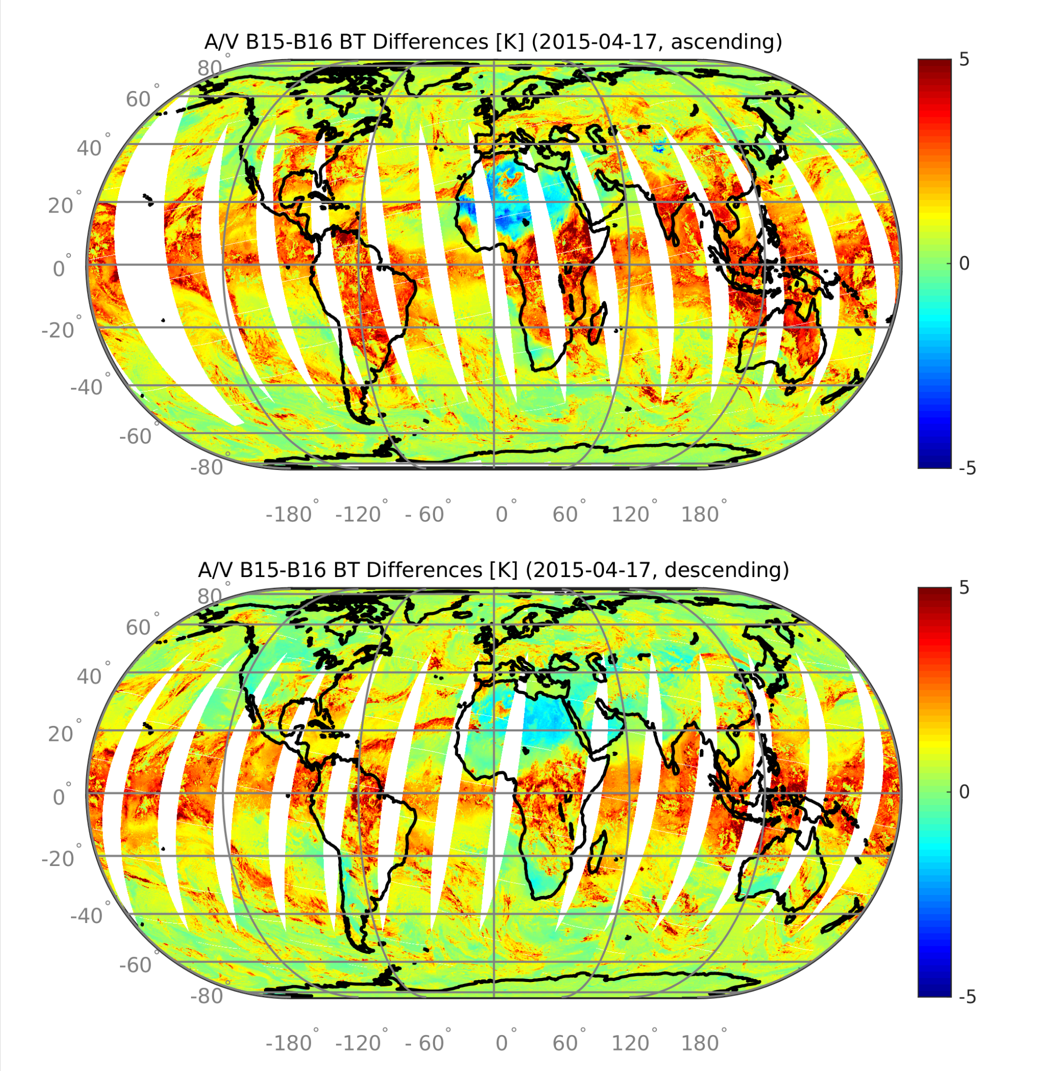

Differences of AIRS/MODIS minus AIRS/VIIRS BT Differences

Global Statistics (240 AIRS granules) of BTD [K]

	mean	stdev	rms
MODIS B31-B32 BTD	0.779	0.950	1.228
VIIRS M15-M16 BTD	0.957	1.036	1.411

Blue (negative values)
→ VIIRS split-window BTD are larger
→ offer increased atmospheric signal due to wider SRFs

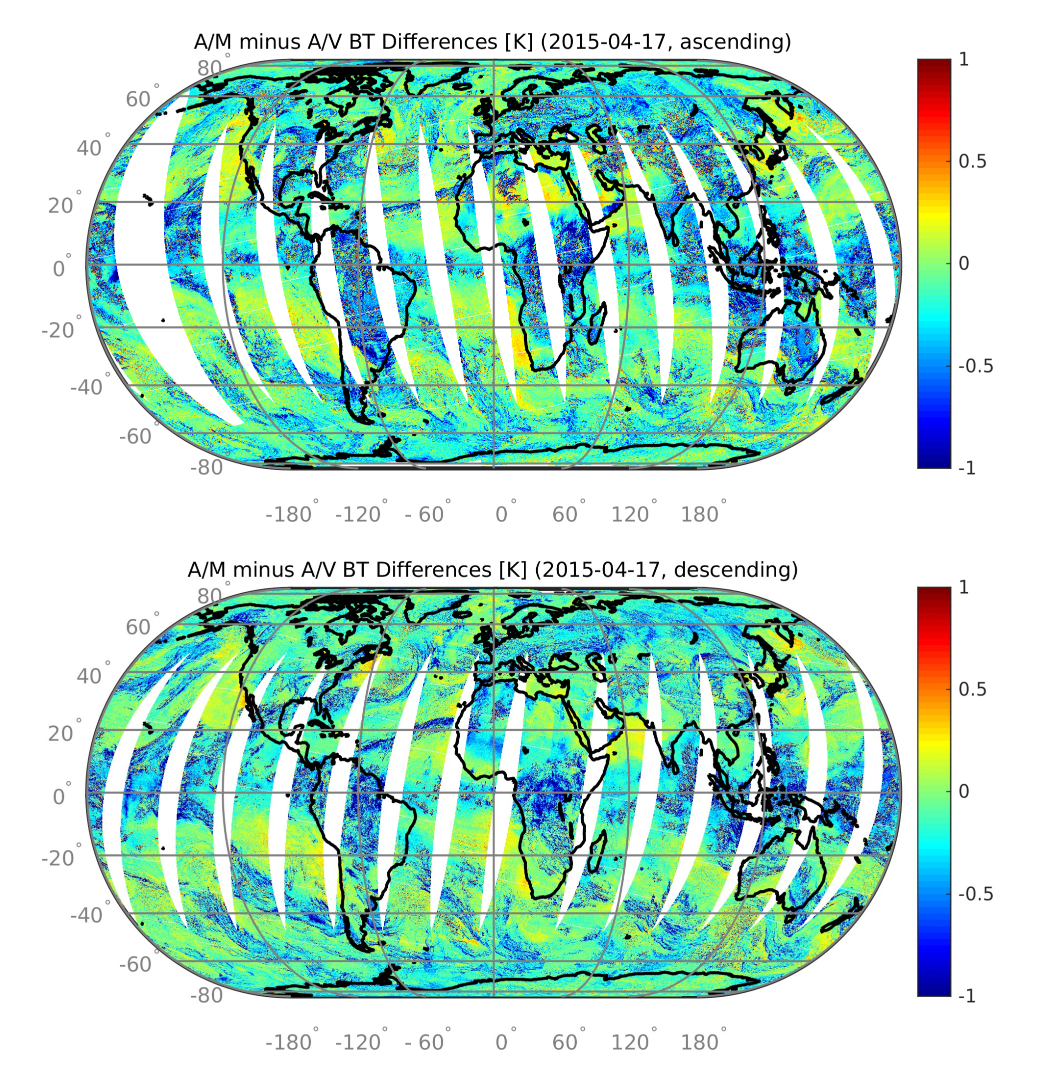

Future Plans

- Continue to maintain the NOAA-20 and S-NPP FSNRAD products
- Document Single-FOV uncertainty estimate in FSNRAD V2 ATBD and the undergoing FSNRAD V2 publication.
- Add pixel-level uncertainty estimates for each band to future versions of product files.
- Testing out the possible use of NOAA-20/CrIS for patching up missing S-NPP FSNRAD bands during the CrIS Side 1&2 MW/LW failing and restoring periods
- Possible study to create high-resolution CERES OLR data
  - [VIIRS Split Window+VIIRS/CrIS fusion]/[CERES OLR] product fusion using the FSNRAD 14.4, 13.3, 8.2, and 6.7 m$\boldsymbol{\mu}$ channels respectively (Lee et al., 2007) in the k-d tree search produces CERES OLR at VIIRS spatial resolution
    - Lee, H., A. Gruber, R. G. Ellingson, and I. Laszlo, 2007: Development of the HIRS Outgoing Longwave Radiation Climate Dataset. *J. Atmos. Oceanic Technol.*, **24**, 2029–2047, https://doi.org/10.1175/2007JTECHA989.1.

References:

- Foster, M. J., C. Phillips, A. K. Heidinger, E. E. Borbas, Y. Li, W. P. Menzel, A. Walther, and E. Weisz, **2023**: PATMOS-x Version 6.0: 40 Years of Merged AVHRR and HIRS Global Cloud Data. *J. Climate*, 36, 1143–1160, https://doi.org/10.1175/JCLI-D-22-0147.1
- Weisz, E. and W. P Menzel, **2022**: Tracking atmospheric moisture changes in convective storm environments using GEO ABI and LEO CrIS data fusion. (Rem. Sens. Env. 14(21), 5327; https://doi.org/10.3390/rs14215327
- Weisz, E. and W. P Menzel, **2022**: Monitoring the 2021 Cumbre Vieja Volcanic Eruption Using Satellite Multi-Sensor Data Fusion. (Jour. of Geophys. Res. Atmos., 128, e2022JD037926. https://doi.org/10.1029/2022JD037926
- Borbas, E. E., E. Weisz, C. Moeller, W. P. Menzel, and B. A. Baum, **2021**: Improvement in tropospheric moisture retrievals from VIIRS through the use of infrared absorption bands constructed from VIIRS and CrIS data fusion, *Atmospheric Measurement Techniques*, 14, 1191–1203, https://doi.org/10.5194/amt-14-1191-2021
- Smith Sr, William & Zhang, Qi & Shao, M. & Weisz, E.. **2020**. Improved Severe Weather Forecasts Using LEO and GEO Satellite Soundings. Journal of Atmospheric and Oceanic Technology. 37. http://doi.org/10.1175/JTECH-D-19-0158.1
- Weisz, E., and W. P. Menzel, **2020**: An Approach to Enhance Trace Gas Determinations through Multi-Satellite Data Fusion, J. Appl. Remote Sens.,14(4), 044519, http://doi.org/10.1117/1.JRS.14.044519
- Anheuser, J., E. Weisz, and W. P. Menzel, **2020**: Low earth orbit sounder retrieval products at geostationary earth orbit spatial and temporal scales, J. Appl. Remote Sens. 14(4), 048502, http://doi.org/10.1117/1.JRS.14.048502
- Li, Y., B. A. Baum, A. K. Heidinger, W. P. Menzel, and E. Weisz, **2020**: Improvement in cloud retrievals from VIIRS through the use of infrared absorption channels constructed from VIIRS-CrIS data fusion, *Atmospheric Measurement Techniques*, 13, 4035–4049, https://doi.org/10.5194/amt-13-4035-2020
- Weisz, E., and W. P. Menzel, **2020**: An Approach to Enhance Trace Gas Determinations through Multi-Satellite Data Fusion, *J. Appl. Remote Sens.*, 14(4), 044519 (2020), http://doi.org/10.1117/1.JRS.14.044519
- Weisz, E., and W. P. Menzel, **2019**: Imager and sounder data fusion to generate sounder retrieval products at an improved spatial and temporal resolution, J. Appl. Remote Sens. 13(3), 034506, http://doi.org/10.1117/1.JRS.13.034506
- Weisz, E., B. A. Baum, and W. P. Menzel, **2017:** Fusion of satellite-based imager and sounder data to construct supplementary high spatial resolution narrowband IR radiances. J. Appl. Remote Sens. 11(3), 036022, http://doi.org/10.1117/1.JRS.11.036022

The End

Cloud Application

(Li et al. 2020) used the 6.7 and 13.3 μm CrIS+VIIRS fusion bands in CLAVR-X, the NOAA operational cloud processing package. They demonstrated that the fusion radiancies improved cloud parameters, *like cloud mask (polar regions), type/phase, and cloud height for all latitudes.*

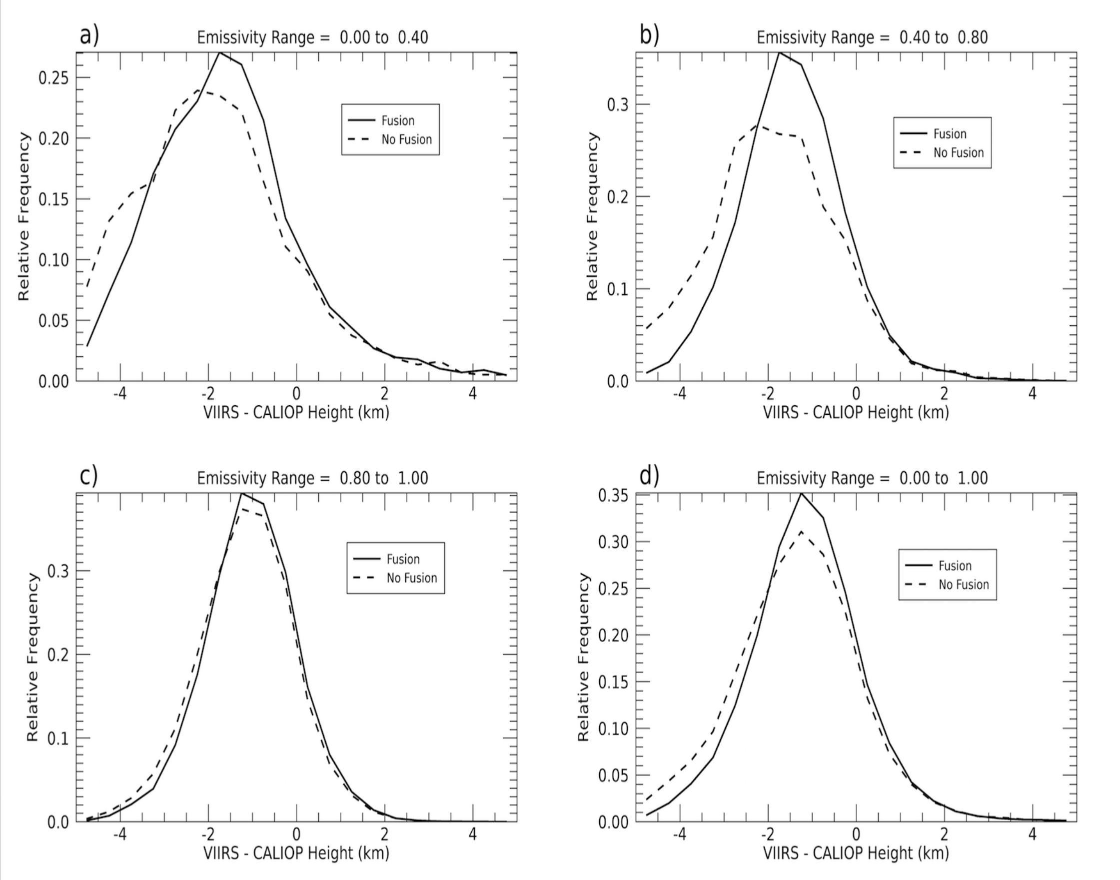

Bias distribution of cloud top height of ice phase clouds between S-NPP VIIRS and CALIPSO/CALIOP for emissivity range a) 0 to 0.4; b) 0.4 to 0.8; c) 0.8 to 1.0; and d) 0 to 1.0. Solid and dashed lines indicate data with/without fusion channels.

Significant improvement is found for all ice cloud emissivities but especially for semi-transparent ice clouds, when the spectral information is used what the FUSION products provide.

Case study
(over land) on 4/17/2015

MODIS granule: at 0805 UTC

VIIRS granules: at 0754 and 0800 UTC

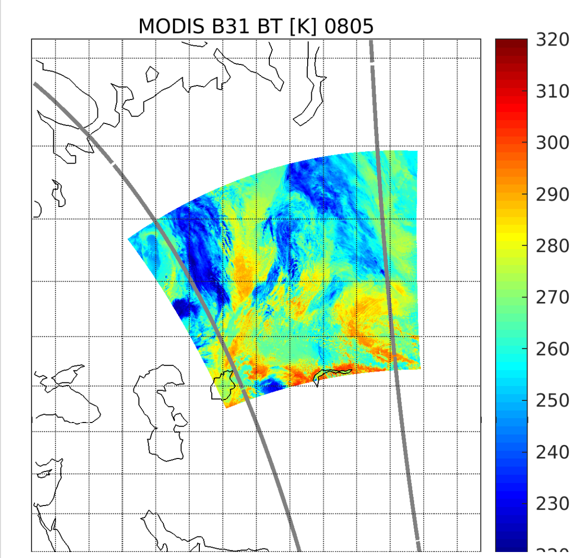
MODIS B31 BT [K] 0805
320
310
300
290
280
270
260
250
240
230

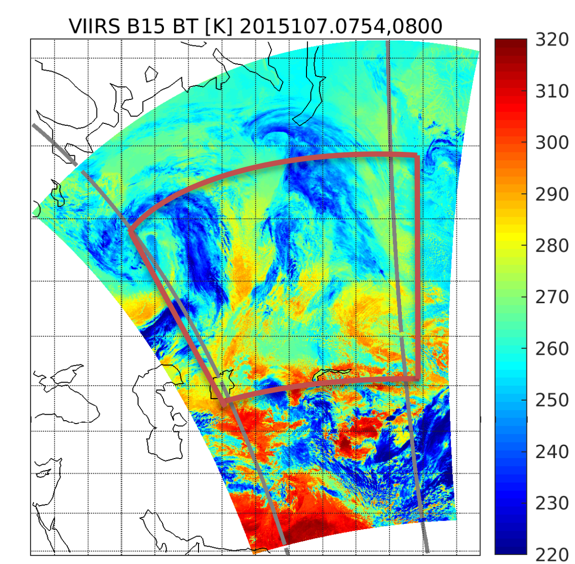
VIIRS B15 BT [K] 2015107.0754,0800
320
310
300
290
280
270
260
250
240
230
220

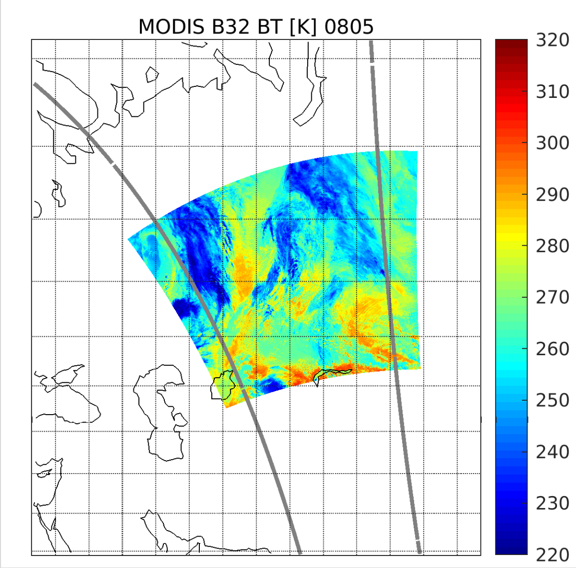
MODIS B32 BT [K] 0805
320
310
300
290
280
270
260
250
240
230
220

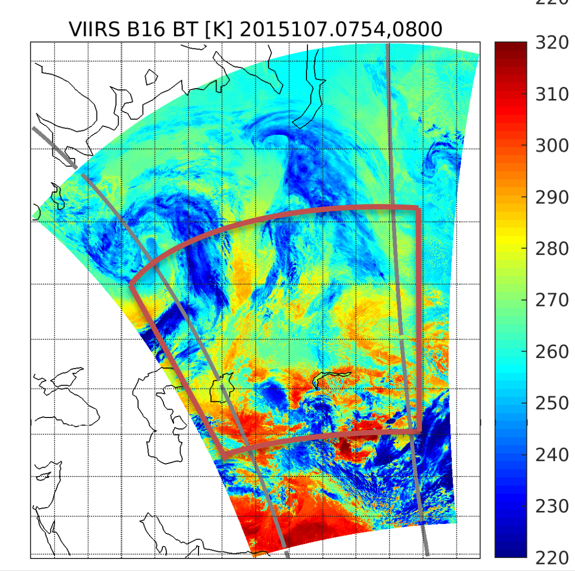
VIIRS B16 BT [K] 2015107.0754,0800
320
310
300
290
280
270
260
250
240
230
220

Predictor 1

MODIS B31 – B32 BT Diff [K]

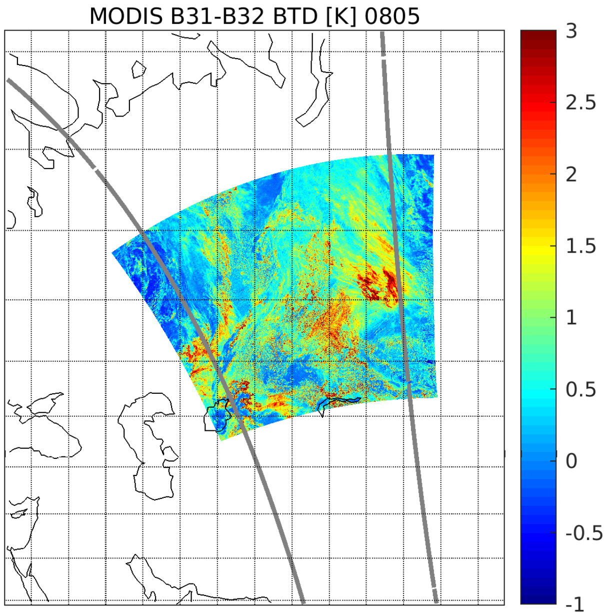

VIIRS M15 – M16 BT Diff [K]

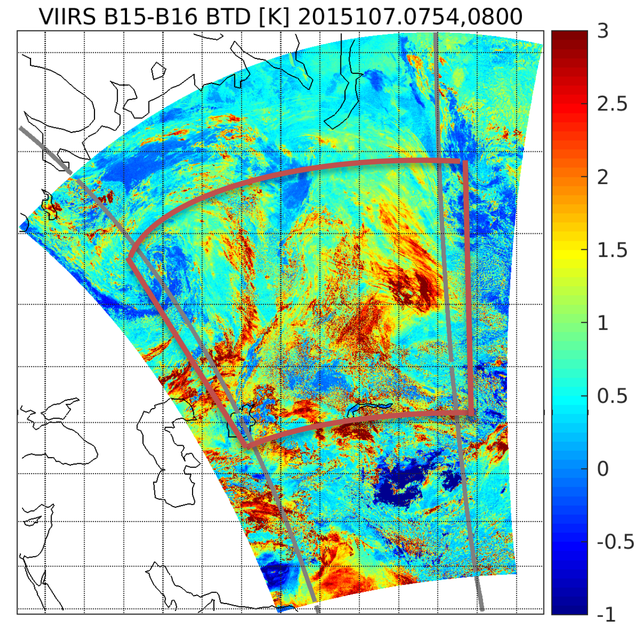

Predictor 2 & 3

Band M15 Observed – Fusion BT [K]

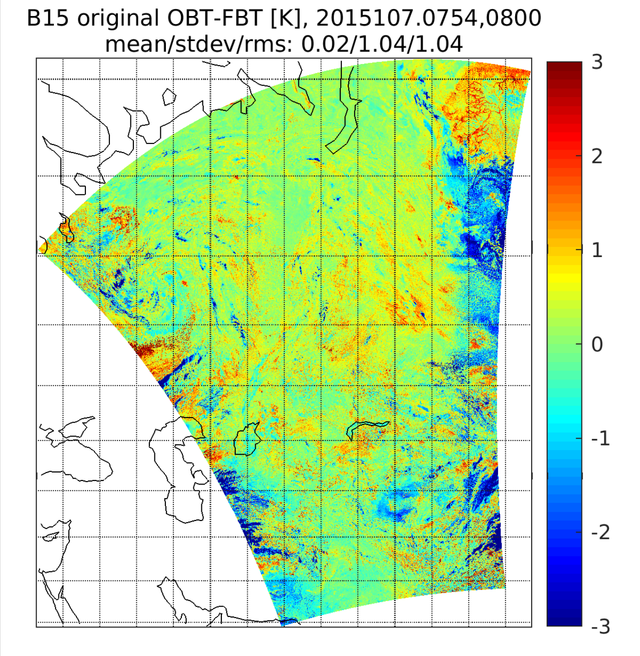

Band M16 Observed – Fusion BT [K]

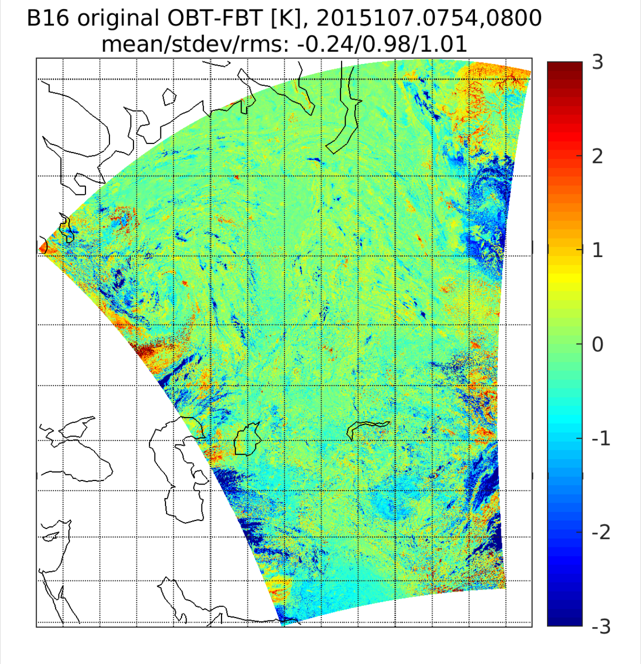

*This data includes the FSNRAD product files.

Band 27 MODIS/AIRS and VIIRS/CrIS Fusion OBT-FBT [K]

MODIS/AIRS OBT-FBT [K]

VIIRS/CrIS OBT-FBT [K]

Original O-F BTs

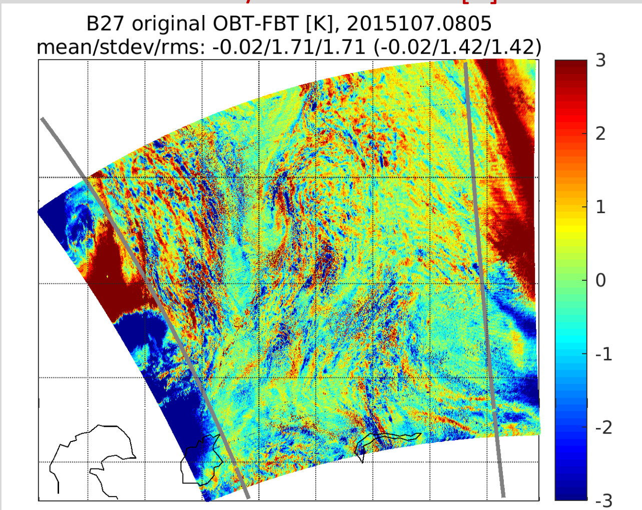

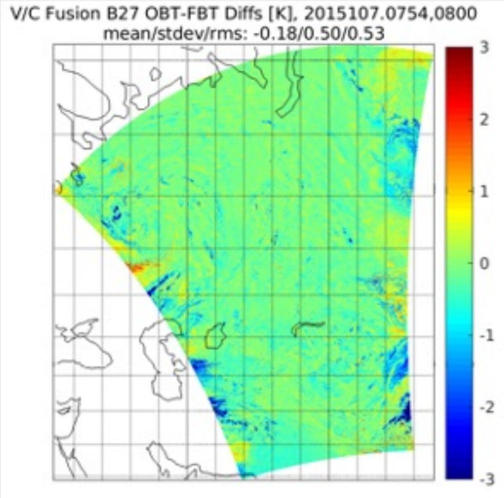

Full granule

Estimated O-F BTs

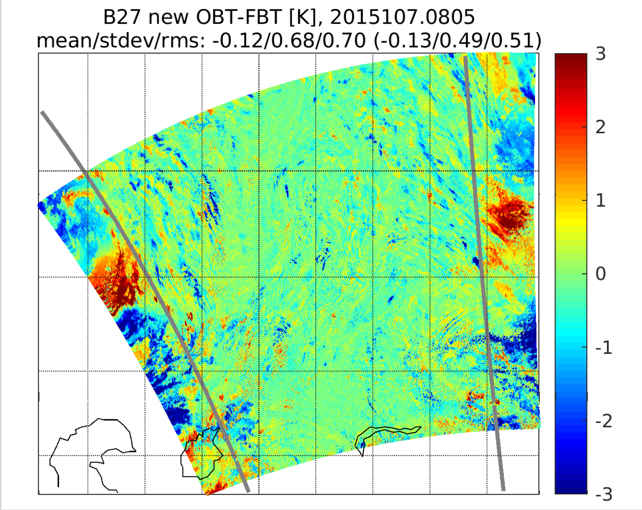

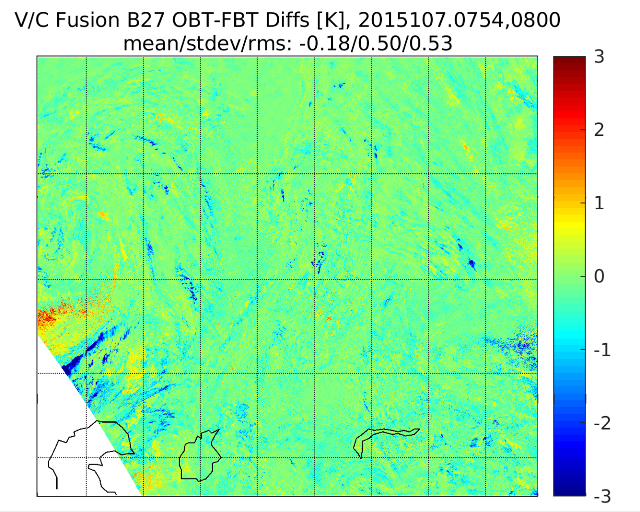

Subset

Band 33 MODIS/AIRS and VIIRS/CrIS Fusion OBT-FBT [K]

MODIS/AIRS OBT-FBT [K]

VIIRS/CrIS OBT-FBT [K]

Original O-F BTs

B33 original OBT-FBT [K], 2015107.0805
mean/stdev/rms: -0.25/1.07/1.10 (-0.18/0.90/0.91)

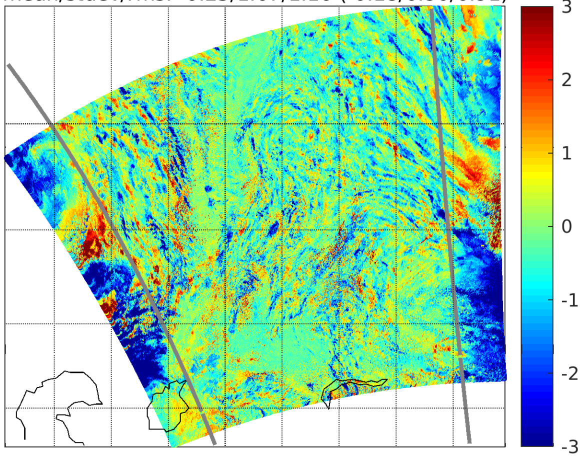

Full granule

V/C Fusion B33 OBT-FBT Diffs [K], 2015107.0754,0800
mean/stdev/rms: -0.53/0.78/0.94

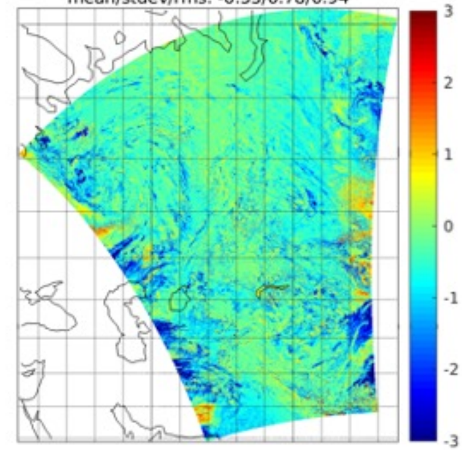

Estimated O-F BTs

B33 new OBT-FBT [K], 2015107.0805
mean/stdev/rms: -0.28/0.87/0.92 (-0.26/0.68/0.72)

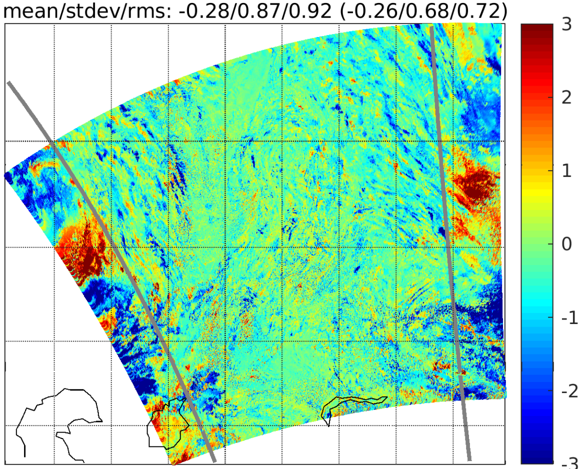

Subset

V/C Fusion B33 OBT-FBT Diffs [K], 2015107.0754,0800
mean/stdev/rms: -0.53/0.78/0.94

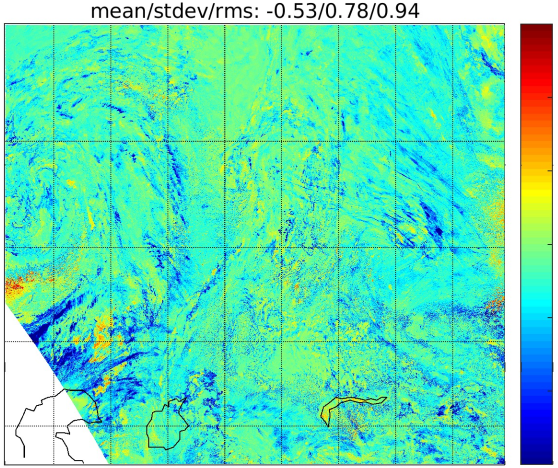

Band 36 MODIS/AIRS and VIIRS/CrIS Fusion OBT-FBT [K]

MODIS/AIRS OBT-FBT [K]

VIIRS/CrIS OBT-FBT [K]

Original O-F BTs

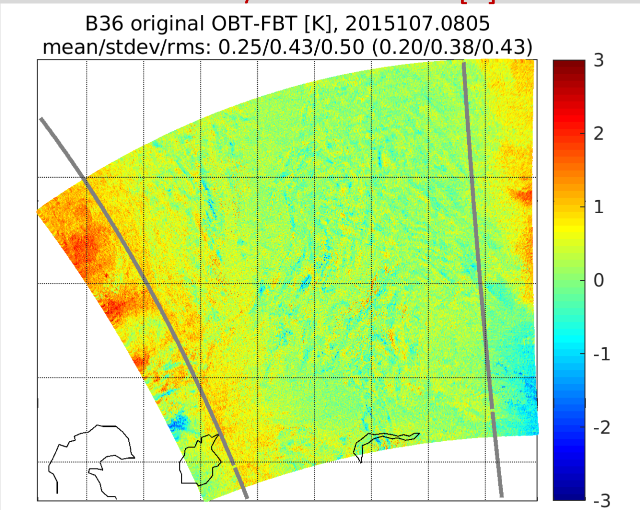

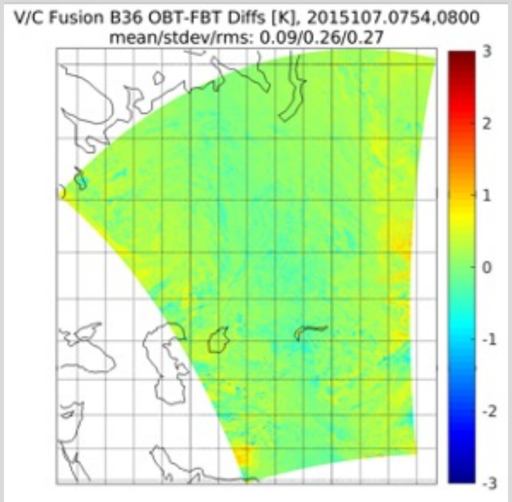

Full granule

Estimated O-F BTs

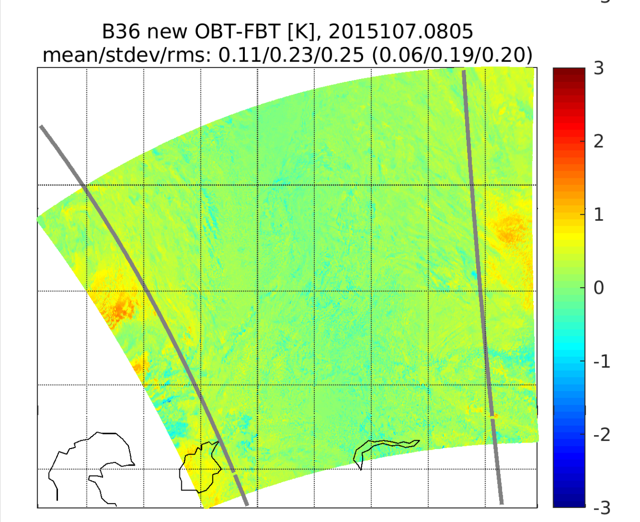

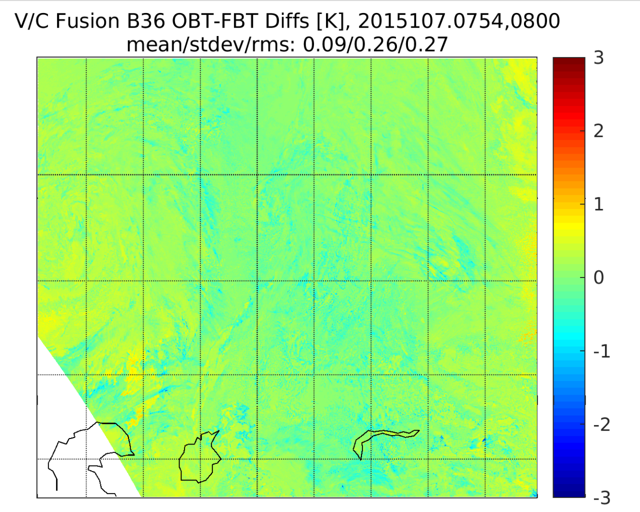

Subset